



Microemulsions formed by PPG-5-CETETH-20 at low concentrations for transdermal delivery of nifedipine: Structural and in vitro study

Guilherme Rodolfo Souza de Araujo^a, Givalda Mendonça da Cruz Macieira^c, Dayane Xavier de Oliveira^c, Saulo Santos Matos^a, Quesia Nery dos Santos^a, Larissa Otubo^b, Adriano Antunes de Souza Araújo^a, Marcelo Cavalcante Duarte^a, Ana Amélia Moreira Lira^a, Rogéria de Souza Nunes^a, Victor Hugo Vitorino Sarmento^{c,*}

^a Department of Pharmacy, Federal University of Sergipe, Av. Marechal Rondon, Jd. Rosa Elze, São Cristóvão, s/n 49100-000 SE, Brazil

^b Instituto de Pesquisas Energéticas e Nucleares, IPEN/CNEN, Cidade Universitária, Av. Prof. Lineu Prestes, 2242, São Paulo, CEP 05508-000 SP, Brazil

^c Department of Chemistry, Federal University of Sergipe, Av. Vereador Olimpio Grande, Sítio Porto, Itabaiana, s/n 49506-036 SE, Brazil

ARTICLE INFO

Keywords:

Microemulsion(s)
Transdermal
Drug Delivery System(s)
Surfactant(s)
Nanotechnology

ABSTRACT

Nifedipine is a potent anti-hypertensive, which is poorly orally bioavailable on account of first-pass metabolism, short half-life, and low water solubility. This study aimed to develop a microemulsified system with low surfactant concentration and to evaluate the influence of microemulsion (ME) phase behavior on skin permeation of nifedipine, as drug model. Thereafter, MEs were obtained using PPG-5-CETETH-20, oleic acid, and phosphate buffer at pH 5.0. The selected MEs were isotropic, with droplet diameters less than 10 nm, polydispersity index < 0.25, and pH between 5.0 and 5.2. MEs presented low viscosity and Newtonian behavior. SAXS results confirmed bicontinuous and oil-in-water (o/w) MEs formation. The presence of the drug promoted only very slight modifications in the ME structure. The MEs presented ability to deliver nifedipine via the transdermal route when in comparison with the control. Nevertheless, the skin permeated and retained amounts from the o/w and bicontinuous formulations did not differ significantly. The ATR-FTIR demonstrated that both formulations promoted fluidization and disorganization of lipids and increased the drug diffusion and partition coefficients in the skin. In conclusion, PPG-5-CETETH-20 MEs obtained proved to be effective skin permeation enhancers, acting by rising the coefficients of partition and diffusion of the nifedipine in the skin.

1. Introduction

Transdermal drug delivery is an important administration route with many advantages over oral or parenteral administrations and is one of the most rapidly advancing areas of novel drug delivery [1,2]. However, the superficial layer of the skin, the stratum corneum, prevents most of the prescriptions from being administered in adequate doses to exert pharmacological action. One option to overcome this barrier and enhance the permeation of drugs into the skin is using microemulsions [3–5].

Microemulsions are systems defined as isotropic, thermodynamically stable, transparent, and low-viscosity, constituted of a mixture of water, surfactants, and oil, classified as water in oil (w/o), bicontinuous, or oil in water (o/w) [6–9]. These systems provide several advantages over conventional formulas which include ease of preparation, increased

lipophilic and hydrophilic drug solubility, enhanced substance permeation through biomembranes, enhanced lipophilic and hydrophilic drug transdermal delivery, and improved stability [1,4,7,10].

Several studies have used the properties of microemulsions to improve the biopharmaceutical characteristics of the most diverse molecules [1,2,4,6,7], including for nifedipine [11,12]. However, such systems are normally prepared with a large amount of surfactant, which is more than 20% of the microemulsion composition. Thus, the search for microemulsion systems stabilized by a low concentration of surfactant becomes interesting, since these substances, when used in large quantities, can be irritating to the skin [3].

The polyoxypropylene (5) polyoxyethylene (20) cetyl alcohol (INCI name: PPG-5-CETETH-20) is a non-ionic surfactant with no unsaturation in its 16-carbon lipophilic chain and a hydrophilic-lipophilic balance of 16, which is able to self-organize into different nanostructures such as

* Corresponding author.

E-mail address: vhsarmento@academico.ufs.br (V.H. Vitorino Sarmento).

<https://doi.org/10.1016/j.colsurfb.2022.112474>

Received 15 December 2021; Received in revised form 13 March 2022; Accepted 19 March 2022

Available online 23 March 2022

0927-7765/© 2022 Elsevier B.V. All rights reserved.

micelles or intermediate structures of mesophases, giving rise to microemulsions or lyotropic liquid crystals [13–15]. In addition, the lack of repulsive electrostatic interactions and the packing in self-assembled structures favor a low surface tension, thus enabling the formation of nanostructures without requiring cosurfactants [16]. This mechanism has been used to implement innovative drug delivery systems for the buccal [17], nasal [18], vaginal [19], and transdermal [20] routes as a technological platform.

Nifedipine is a dihydropyridine-like substance that acts as a calcium channel blocker in the treatment of hypertension, coronary artery angina, and spasm [21,22]. Despite being a potent antihypertensive drug, when administered orally, nifedipine has pharmacokinetic problems that result in extensive first-pass metabolism, short half-life, low bioavailability [12,23,24]. Furthermore, nifedipine has a low molecular weight (346.33 g/mol) and has low water solubility, with a partition coefficient of 2.2, which makes it a promising molecule to be administered via the transdermal route [12,24].

Therefore, this study aims to obtain and investigate microemulsions with different phase behaviors, obtained using low concentrations of PPG-5-CETETH-20 without cosurfactant as a transdermal delivery formulation for lipophilic anti-hypertensive drugs such as nifedipine.

2. Material and methods

2.1. Material

PPG-5-CETETH, marketed as Procetyl AWS®, was acquired from Croda (Campinas, Brazil), Oleic acid (AO), sodium hydroxide (NaOH), and anhydrous monobasic potassium phosphate (KH₂PO₄) from Synth (Diadema, Brazil). Nifedipine was purchased from the HENRIFARMA® (São Paulo, Brazil) and was used as obtained. A Millipore Milli-Q Plus purification system was used to obtain the ultra-pure water. HPLC grade solvents were used in HPLC analysis. Other solvents and reagents used had analytical grades and were acquired from domestic suppliers.

2.2. Phase diagram's construction

To construct the ternary phase diagram, PPG-5-CETETH-20, oleic acid, and phosphate buffer pH 5.0 were used as the surfactant phase, oil phase, and aqueous phase respectively. The diagram was obtained using the titration method [1,6,7]. For this, firstly, mixtures of the surfactant and oil (9:1, 8:2, 7:3, 6:4, 5:5, 4:6, 3:7, 2:8, and 1:9) were prepared and maintained under moderate magnetic stirring. After 20 min of magnetic stirring, increasing volumes of aqueous phase were added slowly while stirring at room temperature.

After each addition of water, the systems obtained were homogenized and the new proportions of each component were calculated and noted, as well as the result of the macroscopic examination of the systems, which were classified as transparent or opaque liquid systems, transparent viscous systems, or phase separation, and the different regions were delimited in the diagram.

2.3. Preparation of microemulsions

After the identification of transparent liquid systems regions in the

phase diagram, the selected systems were prepared. Appropriate amounts of surfactant and oil were homogenized by magnetic stirring for 20 min, followed by slow titration of the aqueous phase under constant homogenization. To produce drug-containing systems, nifedipine was incorporated into the surfactant and oil solution before the addition of the aqueous phase. The final concentration of nifedipine in microemulsions was 2 mg/mL. The entire procedure was performed at room temperature and protected from white light. The proportions of each component are detailed in Table 1.

After production, the samples were kept at rest for 5 days, at room temperature, and protected from light. Then, the systems were characterized using the methodologies described below.

3. Characterization of formulations

3.1. Dynamic light scattering (DLS) and zeta potential

The hydrodynamic radius of the dispersed droplets, the polydispersity index, and zeta potential of the systems were measured by the DLS technique using a Litesizer 500 (Anton Paar) at ambient temperature and without dilution as described by Araujo et al. [1]. The mean ($n = 3$) and standard deviation of the results of size analysis of inert (without nifedipine) and nifedipine-containing systems were statistically compared using one-way analysis of variance (ANOVA), succeeded by Tukey's post test. Data were considered statistically significant at $P < 0.05$.

3.2. Polarized light microscopy

Polarized light microscopy was used to assess the systems' optical characteristics. An optical microscope (Olympus BX-51) was used in conjunction with a digital camera (LC Color Evolution, PL-A662). One droplet of every sample, was deposited on a slide and covered by a cover slip, and then analyzed at 25 °C at a magnification of 20x [1,18]. The morphology of microemulsions inert and containing nifedipine was visualized by transmission electron microscope (JEOL, JEM 2100). The samples were prepared with a drop of microemulsion placed on film-coated copper grids and negatively stained with 2% phosphotungstic acid solution followed by drying in dissector before analysis. [25,26].

3.3. Rheological analysis

The rheological analysis was performed in Anton Paar rheometer (MCR-Modular Compact Rheometer-302). The flow test (steady shear rate) was conducted in the range of 0–200 s⁻¹, with cone – plate geometry (diameter 50 mm, cone angle 1° and 96 μm of truncation). Newton's law model was used to adjust the data. The rheological tests were performed on each sample at 25 °C ± 0.2 °C.

3.4. Small angle X-ray scattering (SAXS)

The arrangement of the systems was evaluated under the same conditions described in [5,6]. The analysis was carried out on the D1B-SAXS1 beamline at the Brazilian Synchrotron Light Laboratory

Table 1

Composition of systems, droplet size, polydispersity index (PDI), zeta-potential, rheology behavior, and pH. S, surfactant phase; O, oil phase; A, aqueous phase; D, drug. * Values are shown as mean ($n = 3$) with standard deviation.

System	Composition (%)				Droplet size (nm)*	PDI*	Zeta potential* (mV)	η (mPa.s ⁻¹)	R ²	pH*
	S	O	A	D						
ME80%	18	2	80	–	7.58 ± 0.34	0.235 ± 0.014	0.20 ± 0.07	17.27	0.9998	5.05 ± 0.047
ME80%N	18	2	80	0.2	8.79 ± 0.26	0.240 ± 0.023	-0.20 ± 0.11	16.65	0.9997	5.18 ± 0.054
ME90%	9	1	90	–	9.49 ± 0.28	0.211 ± 0.017	0.02 ± 0.25	4.56	0.9982	5.12 ± 0.097
ME90%N	9	1	90	0.2	9.75 ± 0.79	0.207 ± 0.006	0.34 ± 0.06	2.81	0.9976	5.24 ± 0.077

(LNLS, Campinas, Brazil). This beamline is equipped with a Silicon-W/B4C monochromator ($\lambda = 1499 \text{ \AA}$) and a detector (Pilatus 300k) at a distance of 814 nm, allowing a measurement range of the scattering from 0.15 to 4.0 nm^{-1} . Measurements were performed at 25 °C and under the same conditions. The overall scattering intensity was determined after parasitic scattering (air and unsampled) and slit scatter removal.

3.5. pH

The pH of the selected formulations was analyzed using a previously calibrated digital potentiometer with a glass electrode and a temperature sensor [6]. The tests were carried out at room temperature (25 °C).

4. Drug permeation and retention

4.1. Preparation of skin

In this study, the skin of the outside of the ears of a pig obtained from a local slaughterhouse was used to study the nifedipine permeation. The skin was prepared as described by Carvalho and co-authors (2016) [5]. Therefore, after cleaning the ear, the dorsal skin of the ear was carefully removed with the aid of surgical material, succeeded by the extraction of the residual adipose and muscle tissue. Then, the skin was dermatomed to a thickness of about 550 μm using a dermatometer (TCM 3000, Nouvag) and preserved frozen ($-4 \text{ }^\circ\text{C}$) within polythene bags wrapped with tin foil for up to two weeks before use in the assay.

4.2. In vitro permeation

Dermatomed skin was used in the permeation of Franz cells (diffusion area = 1.77 cm^2). The skin ($n = 3-4$) was placed between the cell compartments, which contained 14 mL of phosphate buffer pH 5.0 with 30% ethanol (solubility of nifedipine 0.5 mg/mL). Then, the donor compartment received 300 μl of microemulsion (600 μg nifedipine) and the cells were sealed. As a control, a solution of nifedipine in propylene glycol at a concentration of 2 mg/mL was used.

At defined times, 1 mL samples of the receptor medium were collected, filtered, and stored in a vial for quantification. Immediately after each collection, the same volume of receptor solution was carefully replaced so as not to form air bubbles between the skin and the medium. The cells were coupled to a thermostat bath to keep the temperature at 37 °C and the receiver medium was magnetically agitated (600 rpm).

After quantification, the accumulated amount of permeated nifedipine was determined by the equation: $Q = C_t \times V_{rc} + \sum V_c \times C_c / A$, where Q is the total amount permeated at time t ($\mu\text{g}/\text{cm}^2$); C_t is the concentration found at time t ($\mu\text{g}/\text{mL}$); V_{rc} is the volume in the receptor compartment (mL); V_c is the volume removed in previous samples, C_c is the concentration found in these samples and A is the diffusion area (cm^2) [1,18].

The permeation flux (J_{ss} : $\mu\text{g}\cdot\text{cm}^{-2}\cdot\text{h}^{-1}$) was calculated through the slope of the linear portion of the cumulative permeated drug ($(dQ/dt)_{ss}$: μg) versus time (h) graph divided by the permeation skin surface area (A : cm^2) using the equation: $J_{ss} = (dQ/dt)_{ss} / A$, and the lag time was found through x-intercept of the same graph [1,18,27]. The one-way ANOVA test and Tukey's comparisons post-test (GraphPad Prism 5.03) were used to evaluate the data and variations between formulas were considered significant if $p < 0.05$. The permeation kinetics was evaluated from several mathematical models: First order, Higuchi, Korsmeyer-Peppas and Zero order, as described by Malakar, Basu and Nayak (2014) [28].

4.3. Skin Retention assay

The pig ear skin was removed from the Franz cells after 24 h of permeation to determine the amount of nifedipine retained in the skin

layers.

To determine the amount of drug retained in the stratum corneum, each piece of skin (1.77 cm^2) was subjected to the tape stripping technique, which consists of applying successive adhesive tapes on the surface of the stratum corneum under constant pressure. The strips ($n = 14$) were placed together in a falcon-type tube and then 4 mL of methanol were added to promote drug extraction. Tubes were vortexed for 1 min and then sonicated in an ultrasound bath for 30 min 1 mL of this solvent was collected, filtered, and quantified.

After removing the stratum corneum, the remaining skin (epidermis + dermis) was cut into small pieces and added to falcon-type tubes containing 4 mL of methanol, which were homogenized in ultraturax at 10,000 rpm for 1 min, followed by 30 min of sonication. This solution was centrifuged at 5000 rpm, and 1 mL of the solution was collected, filtered, and quantified.

4.4. Quantification of nifedipine

Quantitative analysis of nifedipine was performed in a Shimadzu® liquid chromatography system (Kyoto, Japan) equipped with a degasser (DGU-20A3), two pumps (LC-20 CE), an automatic injector (SIL-20AHT), and a diode array detector (SPD-M20AVP). The mobile phase was an isocratic elution of ultra-purified water and methanol (20:80, v/v). A C-18 column (Phenomenex) with a length and diameter of 250 mm \times 4.6 mm, respectively, and 5 μm mesh size was used. The flow rate was 0.8 mL/min and the injection volume was 20 μl and the ultraviolet detector was fixed at $\lambda = 330 \text{ nm}$ after UV-Vis full wavelength scanning. Under these conditions, the retention time of nifedipine is 5.5 min, with linearity in the concentration range of 0.1–80 $\mu\text{g}/\text{mL}$ ($y = 22853x - 460,5$, $r^2 = 0.9999$).

4.5. Fourier-transform infrared (FTIR) experiments

Snake skin of the Boa constrictor species was donated by Butantã Institute and was used to investigate the permeation enhancing effect of nifedipine-load microemulsions. The skin was cut into circular discs with 3 cm of diameters and hydrated with water for 12 h. After this period, the pieces were dried with filter paper, and inserted into solutions containing the selected microemulsions for a period of 12 h [4,29]. Then, the formulations in the skin sections were removed with running water, dried with filter paper, and placed in a desiccator for at least 24 h. The samples were analyzed by Fourier Transform Infrared Spectroscopy equipped with Attenuated Total Reflectance (ATR-FTIR). Hydrated skin not treated with microemulsion was used as control. ATR-FTIR spectra were obtained using a Perkin-Elmer FTIR System Spectrum BX spectrophotometer. The formulations were characterized with 4 cm^{-1} resolution in 16 sweeps in the frequency range of 4000–700 cm^{-1} at room temperature.

5. Results and discussion

5.1. Construction of the phase diagram and selection of formulations

The ternary phase diagram of PPG-5-CETETH-20, oleic acid, and phosphate buffer at pH 5.0 (Fig. 1) shows five different regions, being two regions (A and B) of Transparent Liquid Systems (TLS), one region of Transparent Viscous Systems, one region of Opaque Liquid System and a Phase Separation region. The results showed that both the surfactant and the oil phase influenced the phase behavior of the ternary system, allowing it to be organized into different types of structures.

The TLS (A) region occurs up to approximately 25% of the aqueous phase, remaining fluid and transparent liquid over 35% of surfactant and supporting the oil phase up to 60%. In the region between 25% and 75% of the aqueous phase, the presence of transparent systems with high apparent viscosity is observed, followed by a new region (B) of transparent liquid (a region greater than 75% of water and up to 5% of the oil

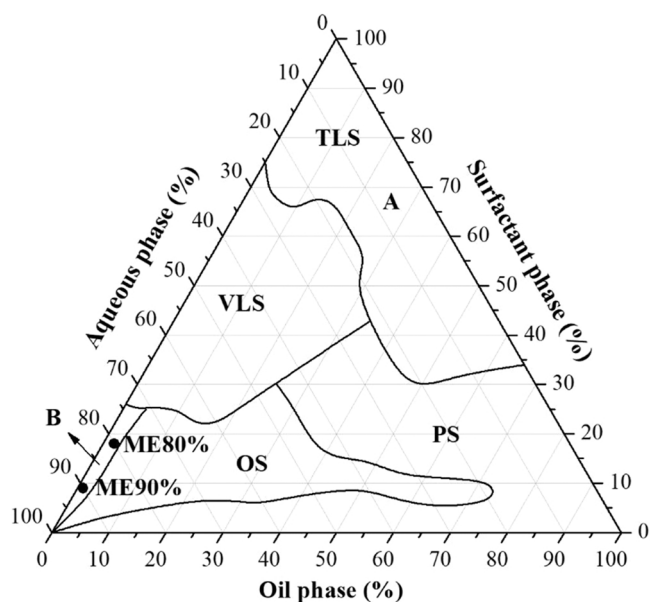


Fig. 1. Ternary phase diagrams for PPG-5- CETETH-20, Oleic Acid, and phosphate buffer pH 5.0 as surfactant phase, oil phase and aqueous phase, respectively. TLS, Transparent liquid systems; VLS, Viscous liquid systems; ME, Microemulsion; OS, Opaque systems; PS, phase separation.

phase). This arrangement of the different regions of this ternary diagram is in accordance with the diagrams available in the literature [20,30,31] and indicates that the use of phosphate buffer with pH 5.0 instead of water as an aqueous phase did not affect the system's organization.

Due to the lipophilic characteristic of nifedipine and considering the arrangement of the regions in the diagram, the B region of TLS was selected to produce drug-carried microemulsions because the proportions of components in this region favor the formation of oil-in-water microemulsions. Furthermore, this region contains a low concentration of surfactant, which is generally associated with skin irritation [32].

The highlighted points in the diagram in Fig. 1 indicate the systems selected for the incorporation of nifedipine. These selected systems were produced as described in item 2.3. After 5 days stored the systems were characterized. The composition of each system is shown in Table 1.

6. Characterization of formulations

Microemulsions are dispersions of two immiscible liquids, usually an aqueous and an oily phase, stabilized by the action of a surfactant agent, which maintains the internal phase dispersed in droplets in size up to 200 nm [1,33]. Thus, the structure of the selected formulations was evaluated by dynamic light scattering, polarized light microscopy, and SAXS to confirm their nanometric arrangement.

The dynamic light scattering analysis showed that both blank systems have the hydrodynamic radius of their droplets in the nanometric order, with ME80% being smaller than ME90% ($P < 0.05$). The incorporation of nifedipine, despite causing an increase in droplet radius, the change was not considered statistically significant ($P > 0.05$). Furthermore, the polydispersity index was less than 0.25 for all samples. The zeta-potential of the systems was close to zero, which was expected since the microemulsions studied are formed by PPG-5-CETETH-20, a non-ionic surfactant [13–15]. The droplet size, polydispersity index, and zeta-potential values for each system are described in Table 1.

The systems were also analyzed under polarized light microscopy to assess their optical properties in relation to isotropy or anisotropy. As shown in Fig. S1, all systems present a dark field when subjected to polarized light, characteristic of isotropic behavior. This behavior is expected in microemulsified systems, because of its nanometric size it is

unable to deflect the light beam and generate images [1,34–36]. Transmission electron microscopy revealed that the components of the microemulsions are dispersed in spherical structures, as expected [26]. Images can be seen in the supplemental material (Fig. S2).

The analysis of the rheological profile of a system allows us to assess its viscosity and, consequently, the interaction between sample structures. The shear stress data (τ) were graphically plotted as a function of the shear rate ($\dot{\gamma}$) and are shown in Fig. 2. All systems exhibited a linear dependence of shear stress as a function of the shear rate characteristic of a Newtonian fluid. Microemulsion systems are expected to exhibit Newtonian behavior as a result of small droplet size and low interaction [1,6,7].

The flow behavior of the systems was described using Newton's law for fluids described as $\tau = \eta \dot{\gamma}$, where η is viscosity. Table 1 gives the values of η and R^2 (regression coefficient) for systems. All formulations presented values of R^2 close to 0.99, indicating a good correlation between the experimental data and fit in the theoretic model. It was observed that the viscosity of the systems decreased with the increase in the proportion of the aqueous phase.

The systems were investigated using SAXS scattering to acquire additional data on the organization of the microemulsion's dispersed phase. Fig. 3 presents scattering intensity curves $I(q)$ as a function of vector q for the selected systems, with and without nifedipine. In the case of ME80%, the SAXS pattern presents a first sharp scattering peak followed by a wider peak, which is unusual for a typical microemulsion. These systems are referred to as bicontinuous microemulsions, systems that present domains of aqueous and oil phases intertwined in the form of channels, stabilized by regions of surfactant in the boundary zones between the domains [37].

Furthermore, it is possible to note that after the incorporation of nifedipine, slight changes were detected in the values of the scattering vector q , indicating that there are no few changes in the size of the inert structure or containing nifedipine, as visualized by dynamic light scattering.

Moreover, the ME80% is located close to the TVS, and thus, the organization demonstrated by SAXS may be due to a slight phase transition, which cannot be visualized by polarized light microscopy.

Kaler and co-authors (1983)[38] proposed that bicontinuous microemulsions are based on the disorder of more organized structures, such as liquid crystals, and can exist in regions close to phase transitions and thus, have a degree of disorder lower than a lamellar phase liquid crystal but higher compared to the typical microemulsion.

In fact, when analyzing the viscosity of ME80%, we noticed that it is almost 3.7 times higher than ME90%, indicating that there is greater interaction between its structures, reinforcing the idea of more structured systems. And indeed, the bicontinuous microemulsion has a higher viscosity than the microemulsion o/w [7]. Studies have shown that when the water content rises, the surfactant headgroups become more hydrated and the o/w microemulsions become more spherical, decreasing viscosity compared to the bicontinuous microemulsion [39, 40].

For the formulation ME90%, the SAXS curve profile is typical of microemulsified systems, a wide peak centered on $q \neq 0$, in this case, probably an o/w microemulsion. When nifedipine is added (ME90%N), the broad peak slightly shifts towards reduced q values (Fig. 3), suggesting an expansion of the scattering units' size, which can be attributed due to the incorporation of nifedipine in the internal phase of microemulsion. The increase in droplet size with drug incorporation was also observed by dynamic light scattering technique. The literature reports similar results for drug-loaded and unloaded microemulsions [1,7, 37].

Finally, in both systems, it is possible to notice that after the incorporation of nifedipine, there is an increase in the scattering intensity signal. The signal strength is related to the degree of organization of the sample, where smaller signals indicate less organized systems [14,37]. Thus, we see that the addition of nifedipine to the system results in a

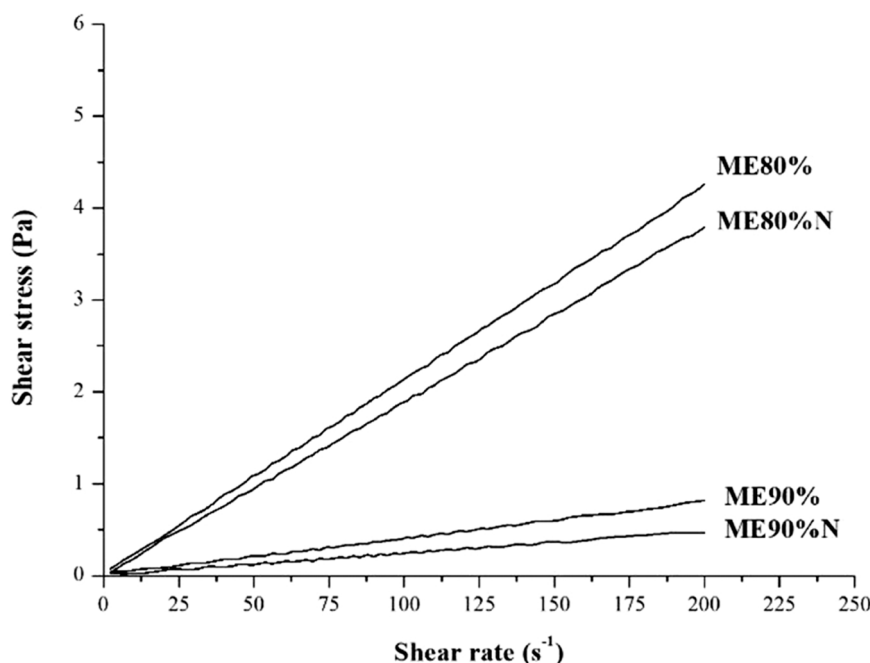


Fig. 2. Rheological behavior (shear stress versus shear rate) of the microemulsion (ME80%, ME80%N, ME90%, and ME90%N).

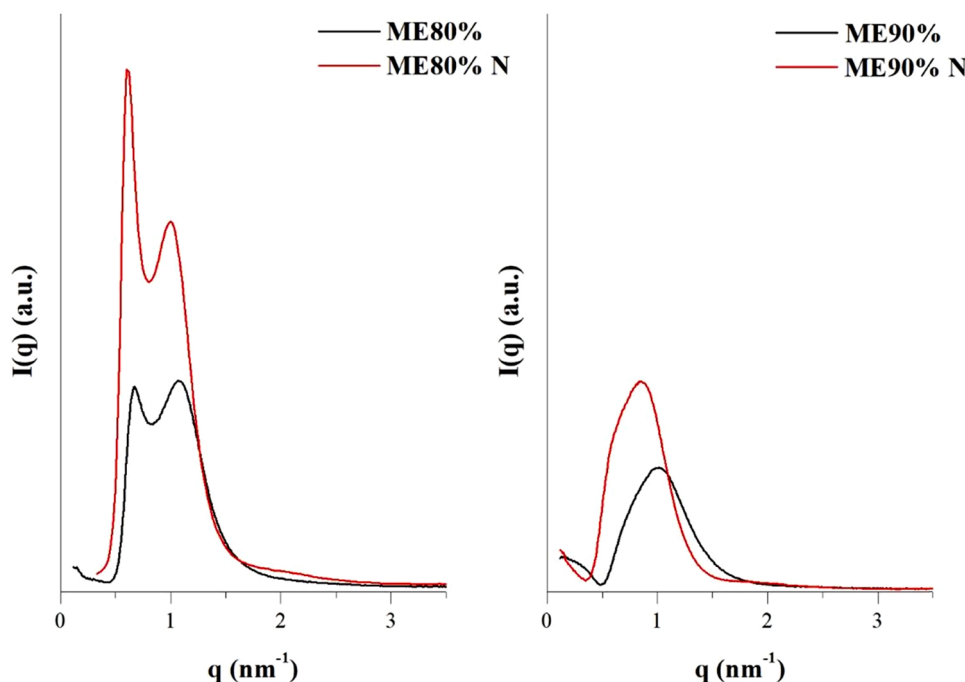


Fig. 3. SAXS analysis for the microemulsion formulations with and without the drug.

slight increase in the organization of the phases of the systems.

All the results of the SAXS analysis are consistent with those found by dynamic light scattering, polarized light microscopy, and rheology analysis, showing that the systems developed have physicochemical characteristics of the microemulsion and the incorporation of nifedipine does not significantly affect these properties.

Regarding the pH of the systems, note that the pH range is between 5.0 and 5.2 (Table 1). The skin has a slightly acidic pH, between 4.6 and 5.8, which contributes to increased protection against bacteria and fungi on its surface. In addition, it has an important buffering capacity, which enables the stratum corneum to be able to tolerate variations in pH from

4 to 7 [41]. Thus, we can highlight that the systems studied are in the pH tolerance range for skin application. Furthermore, the variations suffered by the systems due to the incorporation of nifedipine were unimportant, leading to an indication of thermodynamic stability of the formulations even with the addition of the drug.

7. Drug permeation and retention

Skin permeation tests of nifedipine administered from the developed microemulsions were evaluated using a dermatomed porcine ear bio-membrane model and Franz cell apparatus. Fig. 4A shows the findings of

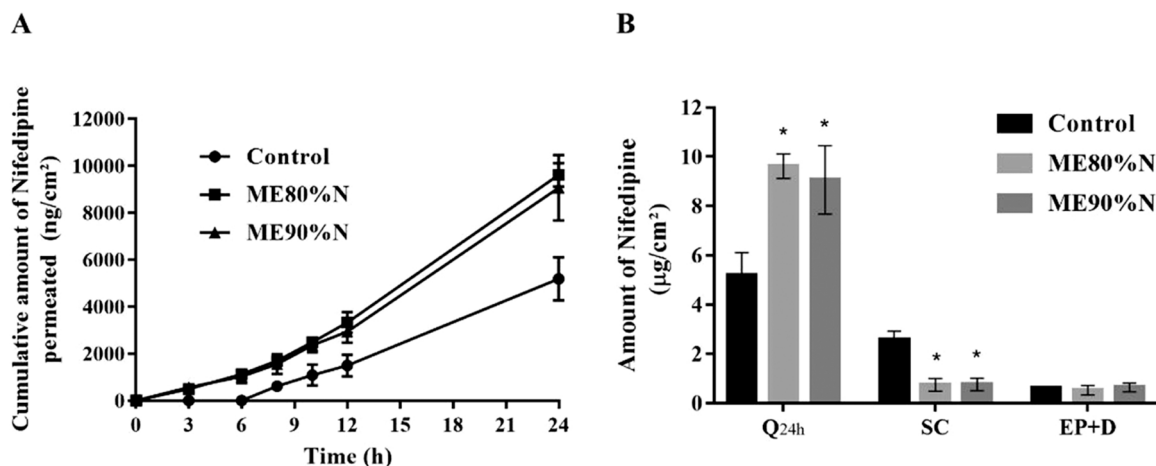


Fig. 4. Permeation profile of nifedipine from microemulsion (ME80%N and ME90%N) (A) and retention of nifedipine in skin layers and in the receptor solution after 24 h (B). * Statistically significant difference ($p < 0.05$) in relation to the control.

the permeation profiles of nifedipine administered from the two systems and a control solution in vitro.

As shown in Fig. 4A and Table 2, the developed systems have shown superior ability to deliver nifedipine via the transdermal route when compared to the control solution. Considering that three systems have the same amount of drug and that the biological membranes used were similar in composition and thickness, it is believed that the difference between performances in the transdermal permeation of nifedipine is due to the composition and structuring of the system, suggesting that microemulsions are acting as permeation enhancers.

Regarding the permeation kinetics models, nifedipine administered from the propylene glycol solution (control group) showed zero-order permeation kinetics, indicating that the permeation flux is being controlled by the skin. However, nifedipine administered from both microemulsions showed a different permeation mechanism, with greater correlation with the Korsmeyer-Peppas model, and a diffusion index greater than 1 ($n > 1$), indicating a complex mechanism of the type super case II diffusion. The linearization data with the different mathematical models can be seen in Table 2.

At the end of the permeation tests, the Franz cells were disassembled, and the skin removed to assess the amount of nifedipine retained 24 h after the administration of the microemulsions. The amount of nifedipine retained and permeated are shown in Fig. 4B and Table 2.

The amount permeated after 24 h of the experiment was greater for microemulsions than for the control solution. However, the nifedipine's total amount in the recipient medium after 24 h from ME80% N and ME90% N did not differ significantly ($P > 0.05$).

Table 2

Permeation, mathematical kinetics models, and retention parameters of nifedipine from the control and selected MEs through the pig skin.

Parameter		Control	ME80%N	ME90%N
Permeation	Jss (ng/cm ² /h)	288.1	484.2	454.8
	Lag time (h)	± 8.82	± 22.82	± 29.14
	ER	6.18	4.4	4.5
Kinetics models (R ²)	First order	–	1.68	1.57
	Higuchi	0.9967	0.9777	0.9790
	Korsmeyer-Peppas(n)	0.9866	0.9064	0.8948
		0.9947	0.9947	0.9887
			(1.44)	(1.34)
Retention	Zero order	0.9968	0.9782	0.9715
	Q _{24h} (µg/cm ²)	5.18	9.61 ± 0.49	9.06 ± 1.39
	SC (µg/cm ²)	± 0.91	1.79 ± 0.80	1.09 ± 0.85
	ED (µg/cm ²)	2.59	0.52 ± 0.19	0.64 ± 0.17
	± 0.33			
	± 0.04			

In the skin retention experiments, the stratum corneum treated with the control had a greater portion of the drug retained ($P < 0.05$). No difference was observed in the amount of drug retained in viable skin between microemulsions and control solution (epidermis and dermis).

The result obtained corroborates the literature, which presents several studies demonstrating the ability of microemulsions to enhance the permeation of drugs through the skin, whether hydrophilic [1,2,4] or lipophilic [7,42].

Interestingly, despite the ME80%N microemulsion present a lower droplet size and containing twice as much oleic acid and surfactant, which are known permeation enhancers [32,43,44], the amount of nifedipine permeated from this system was similar to the amount of drug permeated to from ME90%N. At all times quantified, there was no significant difference between the accumulated amount of nifedipine permeated from the microemulsions ($P > 0.05$).

In several previous studies, microemulsions o/w have presented better performance than microemulsions bicontinuous for different drugs [9,45,46]. In contrast, Machado et al. (2020)[7] found that the microemulsion bicontinuous showed better transdermal delivery, however, the authors used canine skin. In this study, o/w and bicontinuous microemulsions showed similar performance.

Sood et al. (2017)[12] evaluated the transdermal permeation of nifedipine from microemulsions and found values higher than those obtained in this study. However, their formulations contained higher amounts of nifedipine and the biological membrane model used by them was rat skin, which has greater permeability than pig ear skin [47].

Franzé et al. (2018)[23] evaluated the transdermal permeation of nifedipine through human skin. The authors observed that the passive permeation of nifedipine (using a solution of nifedipine in buffer/polyethylene glycol 400 as control) is negligible. Thus, we realize that the microemulsified systems developed are interacting with the stratum corneum, enabling less drug retention, and allowing a greater flow in the permeation of nifedipine and consequently reducing the permeation lag time of this drug.

There are other works in the literature that have investigated the transdermal permeation of nifedipine. However, these articles used complex drug delivery systems such as liposomes [23,48], membranes [49,50] or patch [24], which, despite presenting good permeation values, require several steps to obtain the product.

8. Influence of microemulsion on the stratum corneum permeability

Through the ATR-FTIR technique it is possible to observe the vibration band patterns of the stratum corneum structures such as lipids

and proteins, and changes in these profiles can indicate mechanisms of interactions between the formulations and the skin.

The literature reports the structural similarity between the stratum corneum of human and snake skin [51] and because of that, snake skin was used as a stratum corneum model to investigate permeation mechanisms. This way, the ATR-FTIR band of stratum corneum treated with formulations without (ME80% and ME90%) and with nifedipine (ME80%N and ME90%N), in the region of 2800–3000 cm^{-1} is shown in Fig. 5 and Table 3.

The presence of bands in this region is attributed to the molecular vibrations of the skin lipids [29,41,52]. According to the spectral profiles presented in this region, both the CH_2 asymmetric vibrations (about 2920 cm^{-1}) and the CH_2 symmetric vibrations (about 2850 cm^{-1}) of the skins treated with microemulsions had their bands shifted in relation to the spectrum of untreated snakeskin (control). This change indicates a fluidization of lipids, suggesting a rupture of the stratum corneum [4, 41].

Furthermore, there was a significant increase in the intensity and area of these lipid bands in relation to the spectrum of the control stratum corneum. These results suggest that the components of the formulations (oleic acid or PPG-5-CETETH-20) can be retained by the skin [4,42,53]. This happened in all formulations, inert and loaded with nifedipine.

The elongation profiles of the stratum corneum proteins were also analyzed (region close to wavenumbers 1650 and 1550 cm^{-1} , referring to amides I and II, respectively) and the result is shown in Table 3. It is observed that there was a minimal change in this region, indicating that the formulations do not cause changes in the conformation of skin proteins [54]. Similar results were obtained by Furuishi et al. [54] and Yang et al. [55].

It is known that the mechanisms by which a system with or without permeation enhancer can increase transdermal drug permeation are through interaction with stratum corneum lipids; interaction with intracellular proteins; and/or increased drug partition coefficient in the skin [33]. Based on these mechanisms and on the ATR-FTIR data, it can be verified that the evaluated microemulsions promoted only slight alterations in the protein bands. On the other hand, it was possible to notice that the microemulsions interacted strongly with the skin lipids, generating disorganization and fluidization of the skin and thus enabling an increase in the drug diffusion coefficient through the skin.

Furthermore, since the components of the formulation have been incorporated into the skin, this may be affecting the partition coefficient of nifedipine, as well as aiding in the permeation of the skin. Carvalho et al. [4] evaluated the permeation enhancing mechanism of microemulsions associated with chemical permeation enhancers by ATR-FTIR

Table 3

Comparison of ATR-FTIR spectra from treated and untreated skin to investigate the penetration of nifedipine.

Sample	wavenumber (cm^{-1})			
	CH ₂ stretching		Amide I	Amide II
	Symmetric	Asymmetric		
Control	2862	2924	1652	1540
ME80%	2849	2917	1652	1541
ME80%N	2849	2917	1649	1540
ME90%	2849	2916	1650	1542
ME90%N	2849	2917	1649	1543

using snake skin. The authors found similar results, with microemulsion increasing the diffusion and partition coefficients of zidovudine.

In order to better identify the absorption peaks for each formulation, the second derivative of the FTIR spectrum was used [56]. Fig. 5B shows the spectra of the second derivative of SC, treated with the control (distilled water) or microemulsions selected. It is possible to observe in more detail the changes that occurred in the stratum corneum mentioned earlier, demonstrating clearly which independently of the type of microemulsion tested (bicontinuous or o/w) promoted fluidization and uptake of formulation components, probably promoting an increase in the diffusion coefficient and an increase in the partition coefficient, respectively.

Thus, due to the absence of significant changes in the amide region, indicating that there is no change in protein conformation, it is believed that the permeation-promoting effect is actually due to the disruption of the stratum corneum barrier caused by the incorporation of the microemulsion components to the stratum corneum, resulting in an increase in the diffusion and partition coefficients of nifedipine through the skin. Furthermore, the similarity in the changes in the FTIR profiles after treatment with the different microemulsions justifies the similarity in the skin permeation and retention profile obtained in the Franz cell tests.

9. Conclusion

The present study demonstrates that, under suitable conditions, is possible to incorporate nifedipine in PPG-5-CETETH-20, oleic acid, and phosphate buffer at pH 5.0. The systems obtained were bicontinuous and o/w microemulsions, with isotropy, low viscosity, and Newtonian behavior. These systems are able to reduce the retention of nifedipine in the skin, promoting an increase in its transdermal permeation due to the disruption of the stratum corneum by incorporation of components of microemulsions into the skin and, and probably increase the partition coefficient and diffusion coefficient and of nifedipine. Thus, these

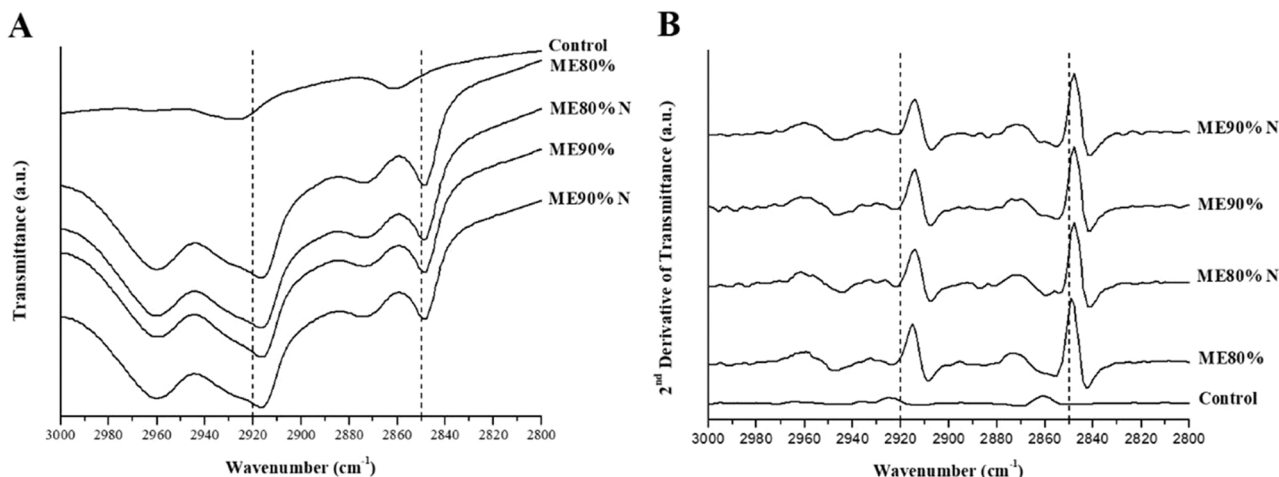


Fig. 5. FTIR spectra of stratum corneum untreated and treated with microemulsions. A) lipid region and B) second derivative of the lipid region.

systems are promising candidates for use in vivo antihypertensive treatment.

CRediT authorship contribution statement

Guilherme Rodolfo Souza de Araujo: Investigation; Formal analysis; Writing – original draft. Visualization; **Givalda Mendonça da Cruz Macieira:** Investigation; Formal analysis; Writing – original draft. **Dayane Xavier de Oliveira:** Investigation. **Saulo dos Santos Matos:** Investigation; Visualization. **Quesia Nery dos Santos:** Investigation; Formal analysis; Visualization. **Larissa Otubo:** Formal analysis; Writing – review & editing. **Adriano Antunes de Souza Araújo:** Resources; Writing – review & editing. **Marcelo Cavalcante Duarte:** Resources; Writing – review & editing. **Ana Amélia Moreira Lira:** Formal analysis; Resources; Writing – review & editing; Supervision. **Rogéria de Souza Nunes:** Resources; Writing – review & editing; Supervision; Project administration. **Victor Hugo Vitorino Sarmento:** Formal analysis; Resources; Writing – review & editing; Supervision; Project administration; Funding acquisition.

Declaration of Competing Interest

The authors declare that they have no known competing financial interests or personal relationships that could have appeared to influence the work reported in this paper.

Acknowledgments

The authors would like to thank CNPq, CAPES, and FAPITEC for funding as well as LNLs SAXS beamtime team for assistance with the measurements and to CLQM (Center of Multi-users Chemistry Laboratories) from Federal University of Sergipe for the analysis assistance. We are also grateful to Anton Paar for dynamic light scattering analysis.

Appendix A. Supporting information

Supplementary data associated with this article can be found in the online version at [doi:10.1016/j.colsurfb.2022.112474](https://doi.org/10.1016/j.colsurfb.2022.112474).

References

- G.R.S. de Araujo, L. de, O. Porfírio, L.A.S. Silva, D.G. Santana, P.F. Barbosa, C. P. dos Santos, N. Narain, V.H.V. Sarmento, R. de, S. Nunes, E. Ting, A.A.M. Lira, In situ microemulsion-gel obtained from bioadhesive hydroxypropyl methylcellulose films for transdermal administration of zidovudine, *Colloids Surf. B Biointerfaces* 188 (2020), 110739, <https://doi.org/10.1016/j.colsurfb.2019.110739>.
- J.A. Alkrad, A.A. Talhouni, In vivo and in vitro study of transdermal application of diclofenac sodium using nonionic microemulsions as colloidal drug delivery systems, *J. Drug Deliv. Sci. Technol.* 43 (2018) 27–33, <https://doi.org/10.1016/j.jddst.2017.08.015>.
- K. Ita, Progress in the use of microemulsions for transdermal and dermal drug delivery, *Pharm. Dev. Technol.* 22 (2017) 467–475, <https://doi.org/10.3109/10837450.2016.1148722>.
- A.L.M. Carvalho, J.A. Silva, A.A.M. Lira, E.D.P. Almeida, R. de, S. Nunes, V.H. V. Sarmento, L.M.C. Veras, J.R. de Almeida Leite, L.B. Leal, D.P. de Santana, Third-generation transdermal delivery systems containing zidovudine: effect of the combination of different chemical enhancers and a microemulsion system, *AAPS PharmSciTech* 19 (2018) 3219–3227, <https://doi.org/10.1208/s12249-018-1160-7>.
- A.L.M. Carvalho, J.A. da Silva, A.A.M. Lira, T.M.F. Conceição, R. de, S. Nunes, R.L. C. de Albuquerque Junior, V.H.V. Sarmento, L.B. Leal, D.P. de Santana, Evaluation of microemulsion and lamellar liquid crystalline systems for transdermal zidovudine delivery, *J. Pharm. Sci.* 105 (2016) 2188–2193, <https://doi.org/10.1016/j.xphs.2016.04.013>.
- A.Á.M. de Sá, E.W.P. dos Santos, M.H. dos, S. Santana, A. de, J. Santos, G.R.S. de Araujo, D.G. Santana, M. de, L.P. de, M. Arguelho, A.M. de, O. e Silva, C.B. Correa, R. de, S. Nunes, V.H.V. Sarmento, A.A.M. Lira, Evaluation of the incorporation of essential oils in microemulsions as a promising formulation in the inhibition of tyrosinase, *Ind. Crop. Prod.* 154 (2020), 112654, <https://doi.org/10.1016/j.indcrop.2020.112654>.
- M. Machado, I.L. Dantas, J.G. Galvão, A.D. Lima, J.K.M. da, C. Gonsalves, C. Gonsalves, E.D.P. Almeida, G.R.S. de Araujo, L.B. Leal, V.H.V. Sarmento, R. de, S. Nunes, A.A.M. Lira, Microemulsion systems to enhance the transdermal permeation of ivermectin in dogs: a preliminary in vitro study, *Res. Vet. Sci.* 133 (2020) 31–38, <https://doi.org/10.1016/j.rvsc.2020.08.009>.
- S.P. Moulík, B.K. Paul, Structure, dynamics and transport properties of micro emulsions, *Adv. Colloid Interface Sci.* 78 (1998) 99–195, [https://doi.org/10.1016/S0001-8686\(98\)00063-3](https://doi.org/10.1016/S0001-8686(98)00063-3).
- J. Zhang, B.B. Michniak-Kohn, Investigation of microemulsion and microemulsion gel formulations for dermal delivery of clotrimazole, *Int. J. Pharm.* 536 (2018) 345–352, <https://doi.org/10.1016/j.ijpharm.2017.11.041>.
- F.F. Sahle, J. Wohlrab, R.H.H. Neubert, Controlled penetration of ceramides into and across the stratum corneum using various types of microemulsions and formulation associated toxicity studies, *Eur. J. Pharm. Biopharm.* 86 (2014) 244–250, <https://doi.org/10.1016/j.ejpb.2013.07.011>.
- D. Thacharodi, K. Panduranga Rao, Transdermal absorption of nifedipine from microemulsions of lipophilic skin penetration enhancers, *Int. J. Pharm.* 111 (1994) 235–240, [https://doi.org/10.1016/0378-5173\(94\)90346-8](https://doi.org/10.1016/0378-5173(94)90346-8).
- J. Sood, B. Sapra, A.K. Tiwary, Microemulsion transdermal formulation for simultaneous delivery of valsartan and nifedipine: formulation by design, *AAPS PharmSciTech* 18 (2017) 1901–1916, <https://doi.org/10.1208/s12249-016-0658-0>.
- F.C. Carvalho, M.D.S. Barbi, M.P.D. Gremião, LC evaluation of in vitro release of AZT from microemulsions, *Chromatographia* 69 (2009) 207–211, <https://doi.org/10.1365/s10337-009-1015-1>.
- S.G. Ferreira, V.S. Conceição, N.S. Gouveia, G.S. Santos, R.L.C. Santos, A.A.M. Lira, S.C.H. Cavalcanti, V.H.V. Sarmento, R.S. Nunes, An environmentally safe larvicide against *Aedes aegypti* based on in situ gelling nanostructured surfactant systems containing an essential oil, *J. Colloid Interface Sci.* 456 (2015) 190–196, <https://doi.org/10.1016/j.jcis.2015.06.012>.
- B. Fonseca-Santos, A.M. dos Santos, C.F. Rodero, M.P. Daflon Gremião, M. Chorilli, Design, characterization, and biological evaluation of curcumin-loaded surfactant-based systems for topical drug delivery, *Int. J. Nanomed.* 11 (2016) 4553–4562, <https://doi.org/10.2147/ijn.s108675>.
- V.H.V. Carvalho, L.A. Sarmento, M.S. Chiavacci, M.P.D. Barbi, Gremião, Development and in vitro evaluation of surfactant systems for controlled release of zidovudine, *J. Pharm. Sci.* 99 (2010) 2367–2374, <https://doi.org/10.1002/jps.22005>.
- B. Fonseca-Santos, B.V. Bonifácio, T.M. Baub, M.P.D. Gremião, M. Chorilli, In-situ gelling liquid crystal mucoadhesive vehicle for curcumin buccal administration and its potential application in the treatment of oral candidiasis, *J. Biomed. Nanotechnol.* 16 (2019) 1334–1344, <https://doi.org/10.1166/jbn.2019.2758>.
- F.C. Carvalho, M.L. Campos, R.G. Peccinini, M.P.D. Gremião, Nasal administration of liquid crystal precursor mucoadhesive vehicle as an alternative antiretroviral therapy, *Eur. J. Pharm. Biopharm.* 84 (2013) 219–227, <https://doi.org/10.1016/j.ejpb.2012.11.021>.
- R. Salmazi, G. Calixto, J. Bernegossi, M. Aparecido Dos, S. Ramos, T.M. Bauab, M. Chorilli, A Curcumin-loaded liquid crystal precursor mucoadhesive system for the treatment of vaginal candidiasis, *Int. J. Nanomed.* 10 (2015) 4815–4824, <https://doi.org/10.2147/IJN.S82385>.
- H.R. Silva, G.M. Luz, C.Y. Satake, B.C. Correa, V.H.V. Sarmento, G.H. de Oliveira, F.C. Carvalho, M. Chorilli, M.P.D. Gremião, Surfactant-based transdermal system for fluconazole skin delivery, *J. Nanomed. Nanotechnol.* 05 (2014) 1–10, <https://doi.org/10.4172/2157-7439.1000231>.
- C.K. Lee, J.S. Choi, D.H. Choi, Effects of HMG-CoA reductase inhibitors on the pharmacokinetics of nifedipine in rats: possible role of P-gp and CYP3A4 inhibition by HMG-CoA reductase inhibitors, *Pharmacol. Rep.* 67 (2015) 44–51, <https://doi.org/10.1016/j.pharep.2014.08.005>.
- T. Handa, S. Singh, I.P. Singh, Characterization of a new degradation product of nifedipine formed on catalysis by atenolol: a typical case of alteration of degradation pathway of one drug by another, *J. Pharm. Biomed. Anal.* 89 (2014) 6–17, <https://doi.org/10.1016/j.jpba.2013.10.024>.
- S. Franzé, A. Marengo, B. Stella, P. Minghetti, S. Arpicco, F. Cilirzo, Hyaluronan-decorated liposomes as drug delivery systems for cutaneous administration, *Int. J. Pharm.* 535 (2018) 333–339, <https://doi.org/10.1016/j.ijpharm.2017.11.028>.
- V.R. Yasam, S.L. Jakkii, J. Natarajan, S. Venkatachalam, G. Kuppasamy, S. Sood, K. Jain, A novel vesicular transdermal delivery of nifedipine-preparation, characterization and in vitro/in-vivo evaluation, *Drug Deliv.* 23 (2016) 629–640, <https://doi.org/10.3109/10717544.2014.931484>.
- E.D.P. Almeida, L.V. Dipieri, F.C. Rossetti, J.M. Marchetti, M.V.L.B. Bentley, R. de, S. Nunes, V.H.V. Sarmento, M.E.G. Valerio, J.J. Rodrigues Júnior, M.M. Montalvão, C.B. Correa, A.A.M. Lira, Skin permeation, biocompatibility and antitumor effect of chloroaluminum phthalocyanine associated to oleic acid in lipid nanoparticles, *Photo Photodyn. Ther.* 24 (2018) 262–273, <https://doi.org/10.1016/j.pdpdt.2018.10.002>.
- R. Song, G. Shen, Y. Liu, F. Tang, Q. Chen, P. Sun, Preparation and characterization of an oil-in-water microemulsion of thiamethoxam and acetamiprid without organic solvent for unmanned aerial vehicle spraying, *Colloids Surf. A Physicochem. Eng. Asp.* 607 (2020), 125485, <https://doi.org/10.1016/j.colsurfa.2020.125485>.
- B. Das, S.O. Sen, R. Maji, A.K. Nayak, K.K. Sen, Transfersomal gel for transdermal delivery of risperidone: Formulation optimization and ex vivo permeation, *J. Drug Deliv. Sci. Technol.* 38 (2017) 59–71, <https://doi.org/10.1016/j.jddst.2017.01.006>.
- J. Malakar, A. Basu, A. Nayak, Candesartan cilexetil microemulsions for transdermal delivery: formulation, in-vitro skin permeation and stability assessment, *Curr. Drug Deliv.* 11 (2014) 313–321, <https://doi.org/10.2174/1567201810666131211110517>.

- [29] M.B. Brito, G.B. Barin, A.A.S. Araújo, D.P. De Sousa, S.C.H. Cavalcanti, A.A.M. Lira, R.S. Nunes, The action modes of *Lippia sidoides* (Cham) essential oil as penetration enhancers on snake skin, *J. Therm. Anal. Calorim.* 97 (2009) 323–327, <https://doi.org/10.1007/s10973-008-9669-8>.
- [30] N.C. Rissi, S.G.D. Aparecida, M.A. Corrêa, L.A. Chiavacci, Relationship between composition and organizational levels of nanostructured systems formed by Oleth 10 and PPG-5-ceteth-20 for potential drug delivery, *Brazil. J. Pharm. Sci.* 50 (2014) 653–661, <https://doi.org/10.1590/S1984-82502014000300025>.
- [31] F.C. Carvalho, H.R.E. Silva, G.M. Da Luz, M. Da Silva Barbi, D.S. Landgraf, L. A. Chiavacci, V.H.V. Sarmento, M.P.D. Gremião, Rheological, mechanical and adhesive properties of surfactant-containing systems designed as a potential platform for topical drug delivery, *J. Biomed. Nanotechnol.* 8 (2012) 280–289, <https://doi.org/10.1166/jbn.2012.1373>.
- [32] A. Seweryn, Interactions between surfactants and the skin – theory and practice, *Adv. Colloid Interface Sci.* 256 (2018) 242–255, <https://doi.org/10.1016/j.cis.2018.04.002>.
- [33] T. Shukla, N. Upmanyu, M. Agrawal, S. Saraf, S. Saraf, A. Alexander, Biomedical applications of microemulsion through dermal and transdermal route, *Biomed. Pharmacother.* 108 (2018) 1477–1494, <https://doi.org/10.1016/j.biopha.2018.10.021>.
- [34] F.C. Carvalho, M.S. Barbi, V.H.V. Sarmento, L.A. Chiavacci, F.M. Netto, M.P. D. Gremião, Surfactant systems for nasal zidovudine delivery: structural, rheological and mucoadhesive properties, *J. Pharm. Pharm.* 62 (2010) 430–439, <https://doi.org/10.1211/jpp.62.04.0004>.
- [35] D.S. Mahrhauser, H. Kählig, E. Partyka-Jankowska, H. Peterlik, L. Binder, K. Kwizda, C. Valenta, Investigation of microemulsion microstructure and its impact on skin delivery of flufenamic acid, *Int. J. Pharm.* 490 (2015) 292–297, <https://doi.org/10.1016/j.ijpharm.2015.05.056>.
- [36] R.M. Hathout, T.J. Woodman, S. Mansour, N.D. Mortada, A.S. Geneidi, R.H. Guy, Microemulsion formulations for the transdermal delivery of testosterone, *Eur. J. Pharm. Sci.* 40 (2010) 188–196, <https://doi.org/10.1016/j.ejps.2010.03.008>.
- [37] A. Kogan, D.E. Shalev, U. Raviv, A. Aserin, N. Garti, Formation and characterization of ordered bicontinuous microemulsions, *J. Phys. Chem. B.* 113 (2009) 10669–10678, <https://doi.org/10.1021/jp901617g>.
- [38] E.W. Kaler, K.E. Bennett, H.T. Davis, L.E. Scriven, Toward understanding microemulsion microstructure: a small-angle x-ray scattering study, *J. Chem. Phys.* 79 (1983) 5673–5684, <https://doi.org/10.1063/1.445688>.
- [39] D.P. Acharya, P.G. Hartley, Progress in microemulsion characterization, *Curr. Opin. Colloid Interface Sci.* 17 (2012) 274–280, <https://doi.org/10.1016/j.cocis.2012.07.002>.
- [40] Y. Ota, A. Hamada, H. Saito, M. Nakano, Evaluation of percutaneous absorption of midazolam by terpenes, *Drug Metab. Pharmacokinet.* 18 (2003) 261–266, <https://doi.org/10.2133/dmpk.18.261>.
- [41] S.A. Ibrahim, S.K. Li, Chemical enhancer solubility in human stratum corneum lipids and enhancer mechanism of action on stratum corneum lipid domain, *Int. J. Pharm.* 383 (2010) 89–98, <https://doi.org/10.1016/j.ijpharm.2009.09.014>.
- [42] S. Ge, Y. Lin, H. Lu, Q. Li, J. He, B. Chen, C. Wu, Y. Xu, Percutaneous delivery of econazole using microemulsion as vehicle: formulation, evaluation and vesicle-skin interaction, *Int. J. Pharm.* 465 (2014) 120–131, <https://doi.org/10.1016/j.ijpharm.2014.02.012>.
- [43] A. Kogan, N. Garti, Microemulsions as transdermal drug delivery vehicles, *Adv. Colloid Interface Sci.* 123–126 (2006) 369–385, <https://doi.org/10.1016/j.cis.2006.05.014>.
- [44] S. Münch, J. Wohlrab, R.H.H. Neubert, Dermal and transdermal delivery of pharmaceutically relevant macromolecules, *Eur. J. Pharm. Biopharm.* 119 (2017) 235–242, <https://doi.org/10.1016/j.ejpb.2017.06.019>.
- [45] J. Zhang, B. Michniak-Kohn, Investigation of microemulsion microstructures and their relationship to transdermal permeation of model drugs: Ketoprofen, lidocaine, and caffeine, *Int. J. Pharm.* 421 (2011) 34–44, <https://doi.org/10.1016/j.ijpharm.2011.09.014>.
- [46] L.M.P. de Campos Araújo, J.A. Thomazine, R.F.V. Lopez, Development of microemulsions to topically deliver 5-aminolevulinic acid in photodynamic therapy, *Eur. J. Pharm. Biopharm.* 75 (2010) 48–55, <https://doi.org/10.1016/j.ejpb.2010.01.008>.
- [47] G.E. Flaten, Z. Palac, A. Engesland, J. Filipović-Grčić, Ž. Vanić, N. Škalko-Basnet, In vitro skin models as a tool in optimization of drug formulation, *Eur. J. Pharm. Sci.* 75 (2015) 10–24, <https://doi.org/10.1016/j.ejps.2015.02.018>.
- [48] S. Franzè, U.M. Musazzi, P. Minghetti, F. Cilirzo, Drug-in-micelles-in-liposomes (DiMil) systems as a novel approach to prevent drug leakage from deformable liposomes, *Eur. J. Pharm. Sci.* 130 (2019) 27–35, <https://doi.org/10.1016/j.ejps.2019.01.013>.
- [49] D. Thacharodi, K. Panduranga Rao, Collagen-chitosan composite membranes controlled transdermal delivery of nifedipine and propranolol hydrochloride, *Int. J. Pharm.* 134 (1996) 239–241, [https://doi.org/10.1016/0378-5173\(96\)04453-5](https://doi.org/10.1016/0378-5173(96)04453-5).
- [50] D. Thacharodi, K. Panduranga Rao, Rate-controlling biopolymer membranes as transdermal delivery systems for nifedipine: development and in vitro evaluations, *Biomaterials* 17 (1996) 1307–1311, [https://doi.org/10.1016/0142-9612\(96\)88676-5](https://doi.org/10.1016/0142-9612(96)88676-5).
- [51] T. Itoh, J. Xia, R. Magavi, T. Nishihata, J.H. Rytting, Use of shed snake skin as a model membrane for in vitro percutaneous penetration studies: comparison with human skin, *Pharm. Res* 7 (1990) 1042–1047, <https://doi.org/10.1023/A:1015943200982>.
- [52] L. Rubio, C. Alonso, G. Rodríguez, M. Cócera, C. López-Iglesias, L. Coderch, A. De La Maza, J.L. Parra, O. López, Bicellar systems as new delivery strategy for topical application of flufenamic acid, *Int. J. Pharm.* 444 (2013) 60–69, <https://doi.org/10.1016/j.ijpharm.2013.01.034>.
- [53] S. Kumar, M. Zakrewsky, M. Chen, S. Menegatti, J.A. Muraski, S. Mitragotri, Peptides as skin penetration enhancers: mechanisms of action, *J. Control. Release* 199 (2015) 168–178, <https://doi.org/10.1016/j.jconrel.2014.12.006>.
- [54] T. Furuishi, T. Fukami, T. Suzuki, K. Takayama, K. Tomono, Synergistic effect of isopropyl myristate and glyceryl monocaprylate on the skin permeation of pentazocine, *Biol. Pharm. Bull.* 33 (2010) 294–300, <https://doi.org/10.1248/bpb.33.294>.
- [55] D. Yang, C. Liu, D. Ding, P. Quan, L. Fang, The molecular design of drug-ionic liquids for transdermal drug delivery: mechanistic study of counterions structure on complex formation and skin permeation, *Int. J. Pharm.* 602 (2021), 120560, <https://doi.org/10.1016/j.ijpharm.2021.120560>.
- [56] L. Rieppo, S. Saarakkala, T. Närhi, H. Helminen, J. Jurvelin, J. Rieppo, Application of second derivative spectroscopy for increasing molecular specificity of Fourier transform infrared spectroscopic imaging of articular cartilage, *Osteoarthr. Cartil.* 20 (2012) 451–459, <https://doi.org/10.1016/j.joca.2012.01.010>.